Modeling and experimental investigation of the electrochemical hole sizing process

Essam Soliman and Hassan El-Hofy
Production Eng. Dept., Faculty of Eng., Alexandria University, P.O. Box 21544, Alexandria, Egypt
e_soliman@alex.edu.eg

This work presents a model for the orbital electrochemical hole sizing process, using a disc like feeding tool. The model is used to investigate the correlation between different process parameters and process performance measures. Process parameters include orbiting speed, feedrate, and tool diameter and lip height. Performance measures include linear and volumetric removal rates, and hole inaccuracy which is represented by the average roundness errors of hole cross sections and average straightness errors of hole sides. A set of fifteen experiments was conducted using different machining parameters to present a base for verifying the model. Experimental and simulation results were compared and it was found that they exhibit the same pattern. Further simulation of the process model showed that increasing feedrate increases hole inaccuracy, however, increasing orbiting speed decreases hole inaccuracy. Also, it was shown that a range of tool diameter should be avoided to ensure high volumetric removal rate. Moreover, increasing tool eccentricity resulted in increased volumetric and linear removal rates, and increased hole inaccuracy.

تقدم هذه الورقه البحثيه نموذج محاكاه لعمليه الضبط الكهروكيميائى المدارى للثقوب ، باستخدام اداه قطع اسطوانيه يتم تغذيتها داخل الثقب. يستخدم النموذج للربط بين عناصر عمليه التشغيل و عناصر قياس اداء عمليه التشغيل. تشمل عناصر عمليه التشغيل السرعه المداريه للقطع و سرعه تغذيه اداه القطع و نصف قطر و سمك اداه القطع. تشمل عناصر قياس اداء عمليه التشغيل معدلى الازاله الخطى و الحجمى و دقه الثقب الناتج معبرا عنها بخطأى الدوران و الاستقامه للثقب. تم اجراء مجموعه من التجارب للتحقق من النموذج و ثبت ان النتائج العمليه و نتائج محاكاه النموذج تتماثل بشكل عام. اظهرت نتائج محاكاه النموذج ان خفض معدل تغذيه الاداه يقلل من دقه الثقب الناتج فى حين ان زياده السرعه المداريه تزيدها. كما اظهرت ان مدى من نصف قطر الاداه يجب تجنبه لضمان زياده معدل القطع الحجمى. كما ان زياده اللامحوريه تؤدى لزياده معدلى القطع الحجمى و الخطى و تقلل من دقه الثقب الناتج.

Keywords: Electrochemical machining, Hole sizing, Modelling, Simulation

1. Introduction

ElectroChemical Machining (ECM) is a metal removal process in which a DC volt is applied across a gap between a cathode electrode tool and an anode work part. A current passes through the electrolyte filled gap. The work part surface dissolves according to Faraday's law. The only reaction that takes place at the tool surface is gas evolution. The tool surface undergoes no erosion and retains its shape. High current densities involved in ECM results in heating of the electrolyte. High flow rate of electrolyte is necessary to keep its conductivity constant and to dispose machining debris.

The ElectroChemical hole drilling and Sizing (ECS) processes are one class of ECM. They include jet, capillary, and electro-stream drilling. They have many applications, especially in the aerospace, electronics and auto industries [1]. This is due to their ability to machine new hard materials without heat affected zones and residual stresses. Drilling of holes with large aspect ratio is another application of these processes. To enhance these processes, orbiting tools are used (OECS) [2]. Orbiting tools can be stationary or feeding ones. Orbiting and feeding tools result in more efficient flow of electrolyte with minimum electrolyte heating effects. Also, disposal of machining debris is faster, thus avoiding short circuit and gap variation problems.

Considerable research work has been conducted to simulate, control and experimentally enhance the ECS process performance. J. Kozak, et al. [3] developed a two dimensional model for the ECS process. They investigated

the effects of machining parameters such as voltage, flow rate and properties of electrolyte on metal removal rate and current density. Experimental and theoretical results showed that metal removal rate is limited by the heating of electrolyte. Mohen et al. [4] reviewed the different ECS processes. They compared them with other hole drilling operations such as electro-discharge and laser drilling. ECS processes have proven to be better from different comparison points such as aspect ratio and hole surface characteristics. S. Sharma et al. [5] investigated the electrochemical drilling of holes in Inconel super alloys using sodium chloride electrolyte. They created a hole in a multilayered work part by feeding an electrode tool towards it. They measured the hole diameter and hole roundness error at each layer as a measure of hole accuracy. They reported inconsistent variations in hole diameters which they reduced, together with roundness errors of the produced hole sections, to variations in process parameters.

H. Hocheng et al. [6] conducted experimental work to study the electrochemical polishing and brightening of holes using rotating and feeding electrodes. They used different rotating speeds at different feedrates. The authors concluded that an optimum set of machining parameters leads to better surface quality and shorter machining time compared with manual and machine lapping processes. Muasuzawa et al. [7] adopted the use of ECM mate electrode to remove the recast layer produced by wire electrodischarge machining. The use of such tool requires large power supply to provide the necessary current density over the entire electrode area. Low current densities could not produce the required surface quality. J. Kozak, et al. [8] used a rotating tool electrode to ensure adequate electrolyte flow in gap and to eliminate the need for high electrolyte pressure. Using the rotating electrode, pressure changes within the gap were small, which resulted in a more stable machining process.

M.S. Hewidy et al. [9] developed a model for the electrochemical drilling under orbital motion conditions. They conducted an experimental work to verify the model. Experimental and model simulation results were in good agreement. Results showed that using orbital motion enhances the accuracy of the machined hole. They also showed that current spikes due to debris accumulation in the gap diminished resulting in better surface finish. Z. Sadollah et al. [10] used an orbiting ECS electrode for finishing surfaces produced by electrodischarge machining. They noticed a reduction in the surface protrusion height at the flow ports. They also noticed an improvement in surface roughness with the increase of orbiting eccentricity and frequency. H. El-Hofy et al. [11- 12] conducted experimental work to study the effect of different machining parameters on quality of holes produces by the OECM process using both stationary and feeding tools. The parameters included tool lip height, in case of feeding tools, and feedrate. They concluded that using orbiting tools results in good surface finish, low roundness errors and efficient machining.

In the present paper, a model of the OECS process is developed and simulated using orbiting and feeding tools. The model is used for studying the effect of different machining parameters on volumetric and linear removal rate and inaccuracy of machined holes. Experimental work is used to verify the developed model.

2. Process modeling and simulation

Fig. 1 shows a schematic representation of the OECS process. A disc like tool of radius R_T and lip height H_T passes through a hole in a work part to adjust hole dimension. The tool is modeled as a stack of N_T discs each of height h, $H_T = N_T \times h$, fig. 1-a. The work part is modeled as a stack of N_w discs each of the height h. The height of the work part is $H_w = N_w \times h$. The work part is further divided into S_w radial segments, fig. 1-b. The tool and work part are eccentric by a distance E, which is the distance between the geometric center of the hole and that of the tool. The work part rotates at N [RPM]. The tool travels at a feedrate F [mm/rev]. It starts moving from an initial potion where it just engages the work part to a final position where it just exits the work part, as shown in fig. 1-a. The distance traveled by the tool, D, is then given by:

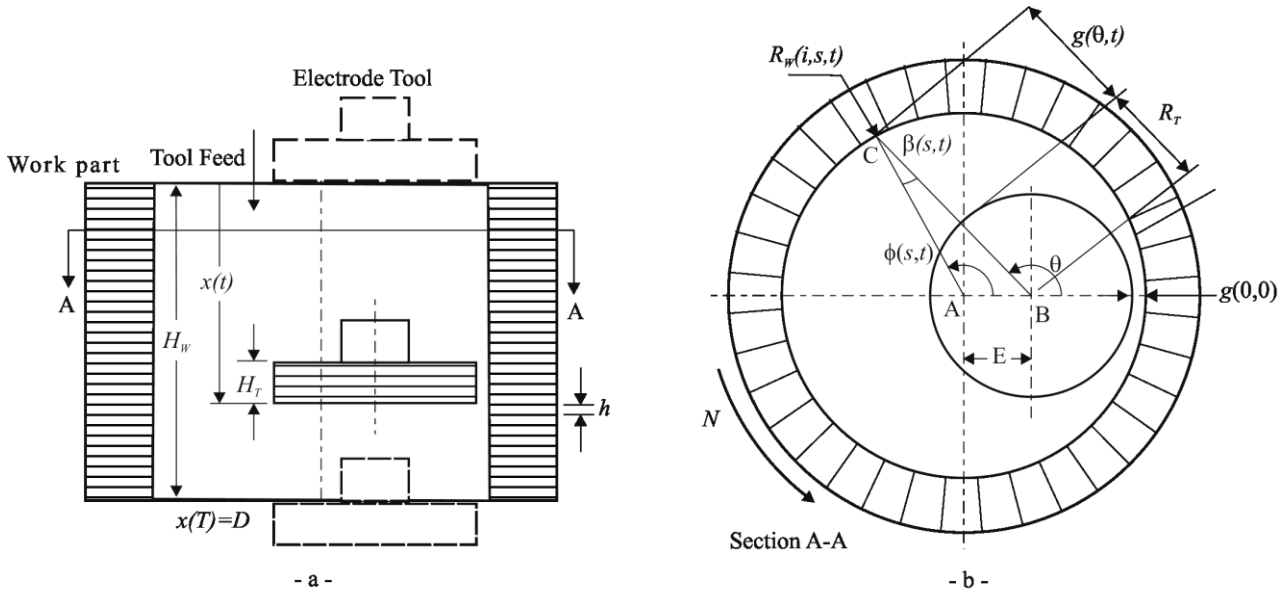

Fig. 1. Model of the orbital electrochemical hole sizing process.

$$D = H_W + H_T . \quad (1)$$

The total machining time T is given by:

$$T = \frac{D}{F \times N} . \quad (2)$$

The axial position of the tool, *x(t)* at any time t [sec] is calculated using the following equation:

$$x(t) = F \times N \times t . \quad (3)$$

Then, for each disc i of the tool, a facing disc of the work part j is determined, where i =1 to N_T, and j is between 1 and N_w, depending on the position of the tool. The tool lasts at any position for at least one incremental time step Δt, depending on the feedrate and disc height h. In the present work, Δt and h are selected for each feedrate so that the tool would last at least $5\Delta t$ at each position.

At any point of time t, the distance between a segment s in disc i of the work part and the geometric center of the hole is expressed by the vector $R_W(i,s,t)$. This vector represents the variations in the hole geometry during machining. In the present work, the vector $R_W(i,s,t)$ is updated each time step and previous values of its elements are ignored. This is to save computer memory during simulation. Also, the present work is concerned with the final rather than incremental radius variations. Therefore, the suffix t is redundant.

After machining time t, the segment s, will have an angular position, $\varphi(s,t)$, which is given from the following equation:

$$\varphi(s,t) = 2\pi \times (\frac{N}{60} \times t + \frac{s}{S_w}) . \quad (4)$$

Also, after machining time t, the segment s, will be separated by a gap $g(\theta,t)$, from the tool as shown in fig. 1-b, where θ is the angular position of the gap around the tool. Referring to fig.1-b, and considering triangle ABC, the following relation is obtained;

$$\frac{E}{\sin(\beta(s,t))} = \frac{R_W(i,s,t)}{\sin(\pi-\theta)} = \frac{R_T + g(\theta,t)}{\sin(\theta-\beta(s,t))} . \quad (5)$$

Hence,

$$\sin(\beta(s,t)) = \frac{E\sin(\pi-\theta)}{R_W(i,s,t)} . \quad (6)$$

The gap $g(\theta,t)$ can, then, be given by;

$$g(\theta,t)=\frac{R_W(i,s,t)\times\sin(\theta-\beta(s,t))}{\sin(\pi-\theta)}-R_T\,. \tag{7}$$

The above equation holds only when the following relation is valid, see fig.1-b:

$$\theta=\beta(s,t)+\varphi(s,t)\,. \tag{8}$$

The initial gap $g(0,0)$ is given by:

$$g(0,0)=R_W(i,1,0)-R_T-E\,. \tag{9}$$

An electrolyte with conductivity κ is assumed to completely fill the gap around the tool. Electrolyte flow rate and work part rotation are assumed to result in negligible conductivity variations. A potential of V_E [volts] is applied across the electrode tool and the work part. Consequently, a current $I(i,s,t)$ flows in radial direction from the work part segment s at the disc i towards tool geometric center. It can be approximated by the following equation, which is derived from the model presented in reference [13]:

$$I(i,s,t)=\frac{V_E\kappa h}{\ln(1+g(\theta,t))}\,. \tag{10}$$

Total machining current at any time can then be obtained from the following equation:

$$I=I(t)=\sum_{t=0}^{T}\sum_{i=1}^{N_T}\sum_{s=1}^{S_w}I(i,s,t)\,. \tag{11}$$

During an incremental time period Δt, the volume of material removed at segment s and disc i, $\Delta(i,s,t)$, can be given from the following equation, where A_w is the atomic weight [kg/mole], Z_w is valency, p_w is density [kg/m^3] and F_a is Faraday's constant:

$$\Delta V(i,s,t)=\frac{A_w\cdot I(i,s,t)\cdot\Delta t}{Z_w\cdot\rho_w\cdot F_a}\,. \tag{12}$$

As a result, hole radius at segment s and disc i will be increased by $\Delta R_w(i,s,t)$ which can be given from the following equation:

$$\Delta R_w(i,s,t)=\frac{\Delta V(i,s,t)\cdot S_w}{2\pi\cdot R_w(i,s,t)\cdot h}\,. \tag{13}$$

The increments of all hole segments during total machining time are averaged to obtain the average hole radius increase, ΔR_w, according to the following equation:

$$\Delta R_w=\frac{1}{S_w\cdot N_w}\sum_{i=1}^{N_w}\sum_{s=1}^{S_w}\sum_{t=0}^{T}\Delta R(i,s,t)\,. \tag{14}$$

The rate of increase of hole radius, LRR, is take as a process performance measure as it represents how fast sizing takes place. It is given from the following equation:

$$LRR=\frac{\Delta R_w}{T}\,. \tag{15}$$

Similarly, volume removal rate, VRR, is taken as a conventional measure of process performance, and is given from the following equation:

$$VRR=\frac{1}{T}\sum_{i=1}^{N_w}\sum_{s=1}^{S_w}\sum_{t=0}^{T}\Delta V(i,s,t)\,. \tag{16}$$

Simulation data, stored in the vector $R_w(i,\ s=1,2,\ldots,S_w,T)$ is used to calculate roundness error of the hole at disc i. Roundness errors of the discs are then averaged to give the hole roundness error. Similarly, simulation data stored in the vector $R_w(i=1,2,\ldots,N_w,\ s,\ T)$ is used to calculate the hole straightness error. Standard procedures are used for calculating straightness and roundness errors [14].

Simulation procedure of the model includes the following steps, which are repeated at each point of time during machining:

1. Calculate tool position, using eq. (3), to determine active hole cross sections at which radius variations will take place.
2. Calculate angular position of the work part, eq. (4).
3. For each segment of the hole find the corresponding angular position with respect to tool center, eqs. (5, 6 and 8).
4. Calculate the gap for each segment, eq. (7).
5. Calculate the current for each segment, eq. (9), and total machining current for all active hole cross sections.
6. Calculate corresponding change in each work part segment radius.
7. Stop simulation if the tool exits the work part according to eq. (1). Then calculate LRR and VRR, considering total machining time, eq. (2).
8. Use work part radius data to calculate roundness and straightness errors at each cross section and consequently the overall roundness and straightness errors
9. Increment simulation time and repeat starting with step 1.

The following table provides a nomenclature for simulation parameters. It, also, gives their default values. If Different values are used, they will be given for the corresponding simulation results.

3. Experimental work

The experimental set up is shown schematically in fig. 2. A cylindrical work part with a 16 mm reamed internal hole is used. The height of the work part is 12 mm. The material of the work part is low carbon steel with 0.15% carbon content. The work part is fixed to the chuck of a center lathe using special attachment, which electrically isolate the work part from the center lathe. The tool is a disc like one as shown in the fig. 2-a with 5 mm radius. The lip height of the tool varies from one experiment to another. The tool is fixed to the cross slide of the lathe using a special attachment. The attachment is a Perspex box like electrolyte cell that isolates the tool from the center lathe body. The tool is fed through the work part at different feedrates using the carriage automatic feeding mechanism. The orbital movement of the tool is obtained relatively by rotating the work part at 95 RPM. The minimum machining gap between the tool and the work part is kept 0.75 mm in all experiments. To set the machining gap, the tool was first allowed to touch the work part by moving the cross slide in the inward direction. Touching was detected by closing an electric circuit which, in turns, turns a lamb on. Then, the cross slide was moved outward by 0.75 mm using the 0.05 mm resolution scale shown in fig. 2-b. The tool attachment was precisely set so that the tool is concentric with the lathe spindle in a vertical plane.

A saturated (150 gm/liter) NaCl aqueous solution is pumped into the gap at a rate of 6 liter/min. The flow rate is set for all experiments by adjusting an orifice valve fitted to the out line of the pump. The amount of solution collected during certain period of time is used to calculate flow rate. The pump and valve are not shown in the experimental setup due to irrelevancy. A full wave rectified DC

Table 1
Default simulation parameters

Parameter	Symbol	Value	Parameter	Symbol	Value
Work part height	H_w	12 [mm]	Orbiting speed	N	95 [RPM]
Tool height	H_T	3 [mm]	No. of radial sectors	S_w	90
Work part radius	R_w	8 [mm]	Volt	V_E	21 [volts], 50 Hz
Feedrate	F	0.1 [mm/rev]	Time increment	Δt	0.001 [sec]
Atomic weight	A_w	0.056 [kg/mole]	Conductivity	K	25 [1/Ω/m]
Valency	Z_w	2	Density	p_w	7800 [kg/m^3]
Tool radius	R_T	5 [mm]	No. of work part discs	N_W	120
Disc height	h	0.1 [mm]	Faraday's constant	F_a	96494 [A.sec]
Eccentricity	E	2.25 [mm]	No. of tool discs	N_T	30
Tool position	x	[mm]	Tool travel	D	[mm]
Machining gap	g	[mm]	Machining current	I	[A]
Work radius variation	ΔR_w	[mm]	Machined volume	ΔV	[mm^3]
Volumetric removal rate	VRR	[mm^3/min]	Linear removal rate	LRR	[μm/min]
Work part mass reduction	ΔM	[kg]	Current efficiency	ξ	[%]

voltage, 21 volts equivalent, is applied across the –ve electrode tool and the +ve work part. At the beginning of machining, the front face of the tool is just outside of the work part while at the end of machining, the end face of the tool is outside the work part. This is accomplished using limit switches. Machining time is the time required by the tool to move between switches.

A set of fifteen experiments were conducted to present a base for verifying the model. Five tools with different lip heights were used; 1, 3, 5, 8 and 10 mm. Each tool was fed through the work part at different feedrates; 0.05, 0.1 and 0.5 mm/rev. The work part diameter and weight were measured before and after machining for each experiment. Then, mass reduction of work part, ΔM, is determined. *VRR* and *LRR* are determined by considering machining time of the experiment. Current efficiency was calculated using the following equation:

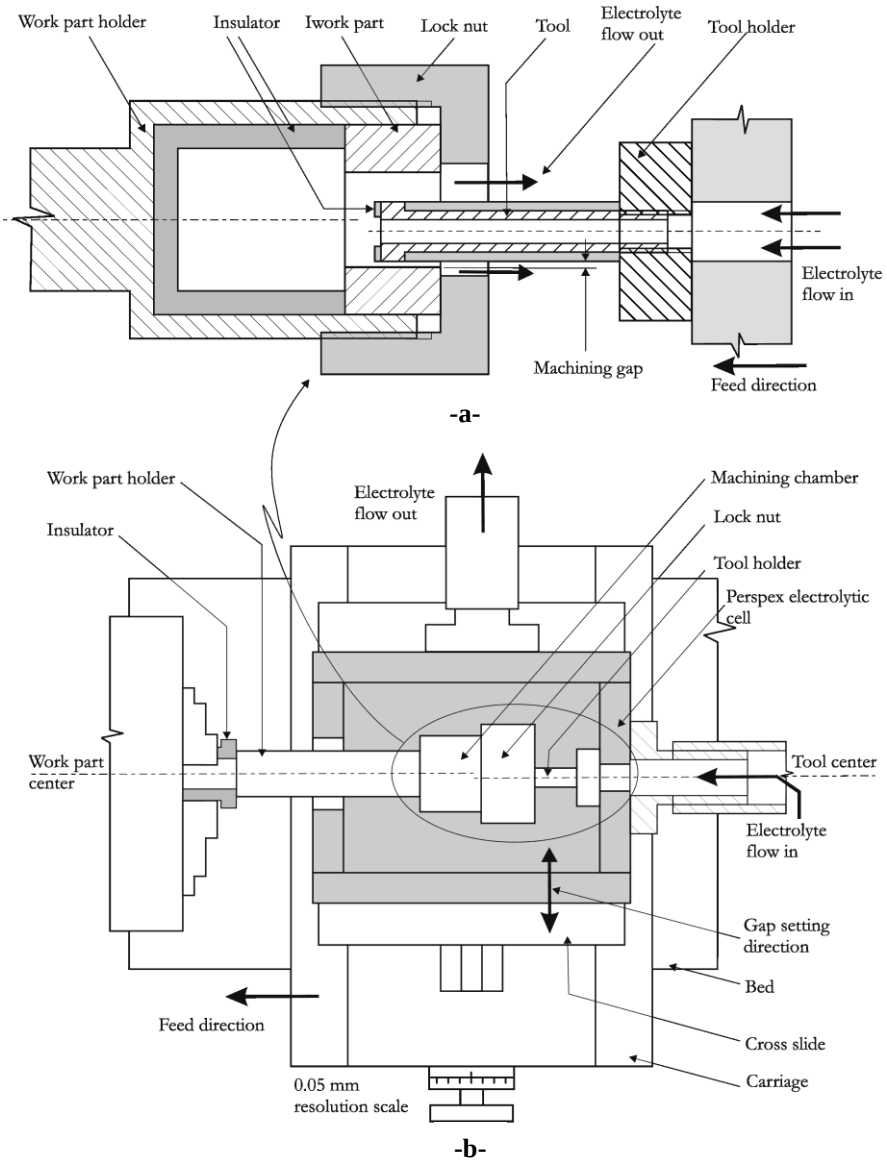

Fig. 2. Schematic diagram of the experimental setup.

$$\xi = \frac{\Delta M}{\rho_w \cdot T \cdot VRR}. \quad (17)$$

Where, ξ is current efficiency and ΔM is change in work part mass after machining.

4. Results and discussions

Fig. 3-a shows the variations of current efficiency, ξ, with tool lip height and feedrate, H_T and F respectively. From the figure, it can be seen current efficiency exceeds 100% in some experiments. This is because a true rectified sine wave is used to apply volt across the machining gap. This was not the case for the experimental machining gap where the rectified signal obtained from the power supply was slightly distorted with little bias. Analyzing and improving the performance of the power supply was outside the scope of the present work. Also, from the figure, it can be seen that current efficiency is above 100% for small values of H_T. Increasing H_T, beyond 3 [mm], does not significantly affect current efficiency. This is because small lip height results in easier flow and less heating and gas evolution of electrolyte. The figure, also, shows that lower F results in higher current efficiency. The F direction is opposite to the electrolyte flow out direction thus higher F presents an obstacle to the electrolyte flow.

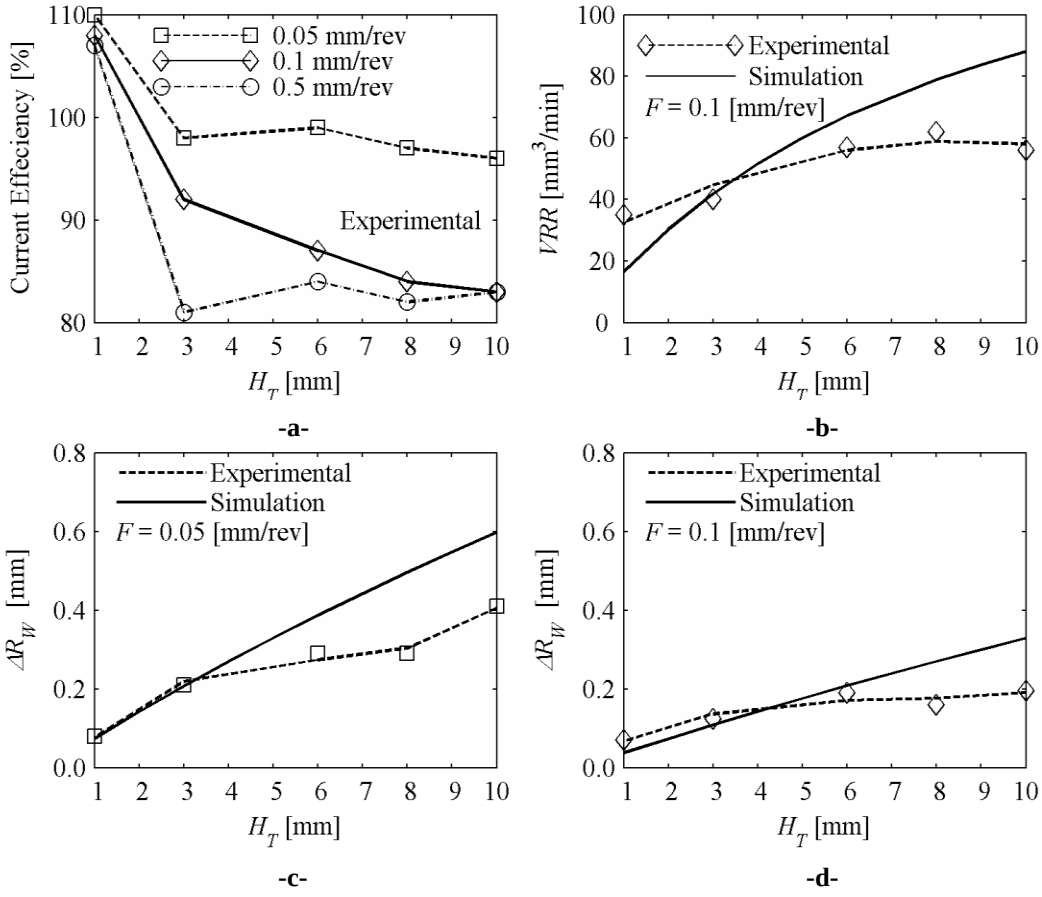

Fig. 3. Effect of tool lip height H_T on current efficiency, ξ, volumetric removal rate, VRR, and hole radius variation, ΔR_W.

The effect of tool lip height, H_T, on volumetric removal rate, *VRR*, is determined experimentally and from model simulation. Results are given in fig. 3-b. From the figure, it can be seen that there is a deviation between the simulation and experimental trends. However, the figure shows that for small H_T the experimental *VRR* is the larger than simulated *VRR*, while for large H_T, simulated *VRR* is larger than experimental *VRR*. This result is a consequence of the result, concerning effect of H_T on current efficiency, obtained in fig. 3-a. Figs. 3-c and 3-d show the effect of tool lip height, H_T, on simulated and experimental hole radius variation, ΔR_W, for 0.05 and 0.1 [mm/rev] feedrates, *F*, respectively. It is clear that increasing H_T results in increased ΔR_W. It is, also, clear that experimental ΔR_W is slightly larger than simulated ΔR_W for small H_T while experimental ΔR_W is smaller than simulated ΔR_W for large H_T. Again, this result is a consequence of the same result obtained in fig. 3-a.

The effect of feedrate, *F*, on volumetric removal rate, *VRR*, and hole radius variation, ΔR_W, is shown in figs 4-a and 4-b respectively. From fig. 4-a, it can be seen that for small *F*, less than 0.3 mm/rev, increasing feedrate results in a considerable increase in *VRR*, about 7%. However, increasing *F* beyond 0.3 mm/rev does not have a significant effect on *VRR*, less than 1%. In general, the effect of *F* on *VRR* is marginal. The effect of *F* on ΔR_W is shown in fig. 4-b, which indicates that increasing the *F* results in less change in ΔR_W. The same trend is exhibited for simulation and experimental results. The experimental ΔR_W is slightly larger than the simulated one due to the increased experimental current efficiency at small H_T , which is 3 mm as indicated in figs. 4-a and 4-b.

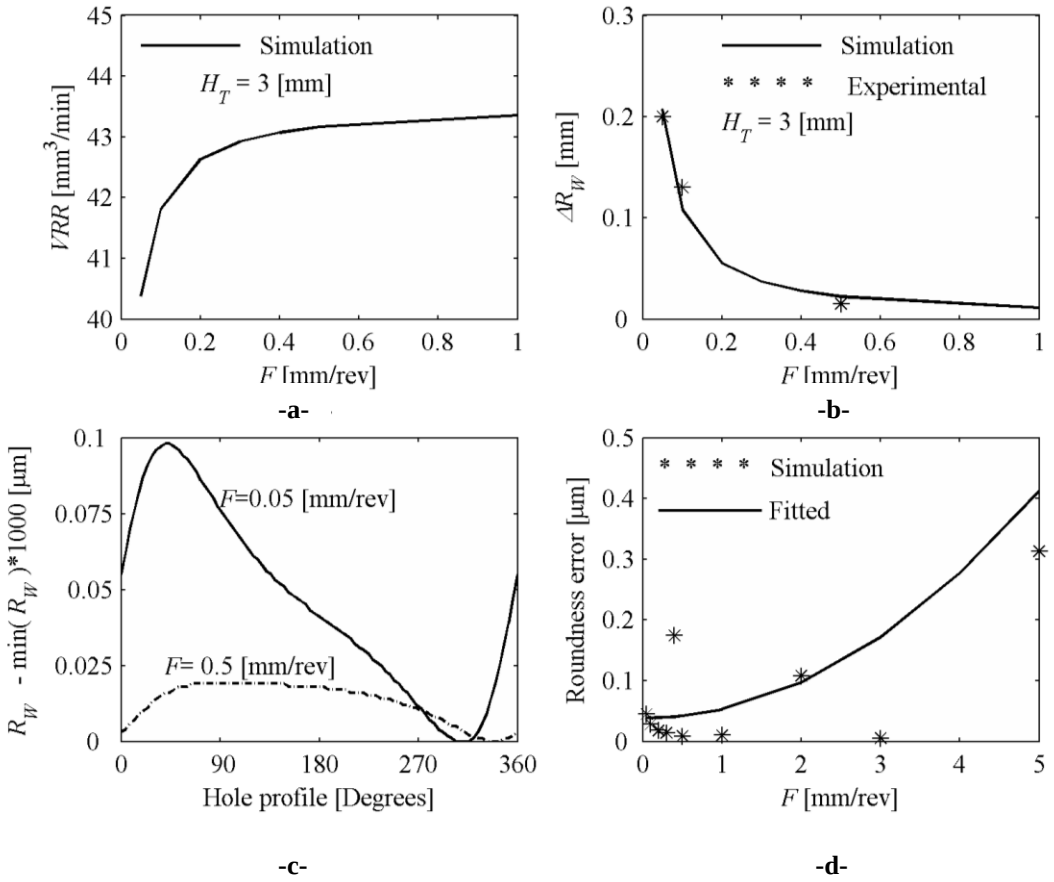

Fig. 4. Effect of feedrate, *F*, on volumetric and linear removal rates, *VRR*, *LRR*, respectively and hole roundness error.

Figs 4-c show normalized R_W variations, which are obtained by subtracting the work part radius at each segment of a cross section from the minimum radius. A cross section that is 12 mm away from the starting machining side of the work part is considered. Two values of F are used; 0.05 and 0.5 mm/rev. Smaller feedrate results in larger normalized R_W variations. This, in turns, results in larger roundness error at smaller F. This can be reduced to the larger changes in R_W at small F as shown in fig. 4-b. However, further increase in F results in dispersed results, as shown in fig. 4-d. This is mainly due to incomplete and non uniform machining of the hole sides at high F. These results are parallel to the experimental results presented in ref. [13].

Fig. 5 shows the variations in the experimental and simulated average machining current over time. Fig. 5-a shows the simulated actual and averaged (filtered) I, for a tool having R_T = 8 mm. The averaging process is obtained by using a 9th low pass filter with 10 Hz cut off frequency. Figs. 5-b, 5-c and 5-d show the simulated and machining currents for three tools with R_T = 1, 3, 7 mm respectively. The figures show that there deviations between experimental and simulation results in terms of the patterns of average I over time. This can be related to stray current effect and the high current efficiency even at low current densities. Also, it is clear that the experimental average I is higher than the simulated one for small H_T while the experimental average I is lower than the simulated one for large H_T. This result is parallel to those results obtained through figs. 3 and 4.

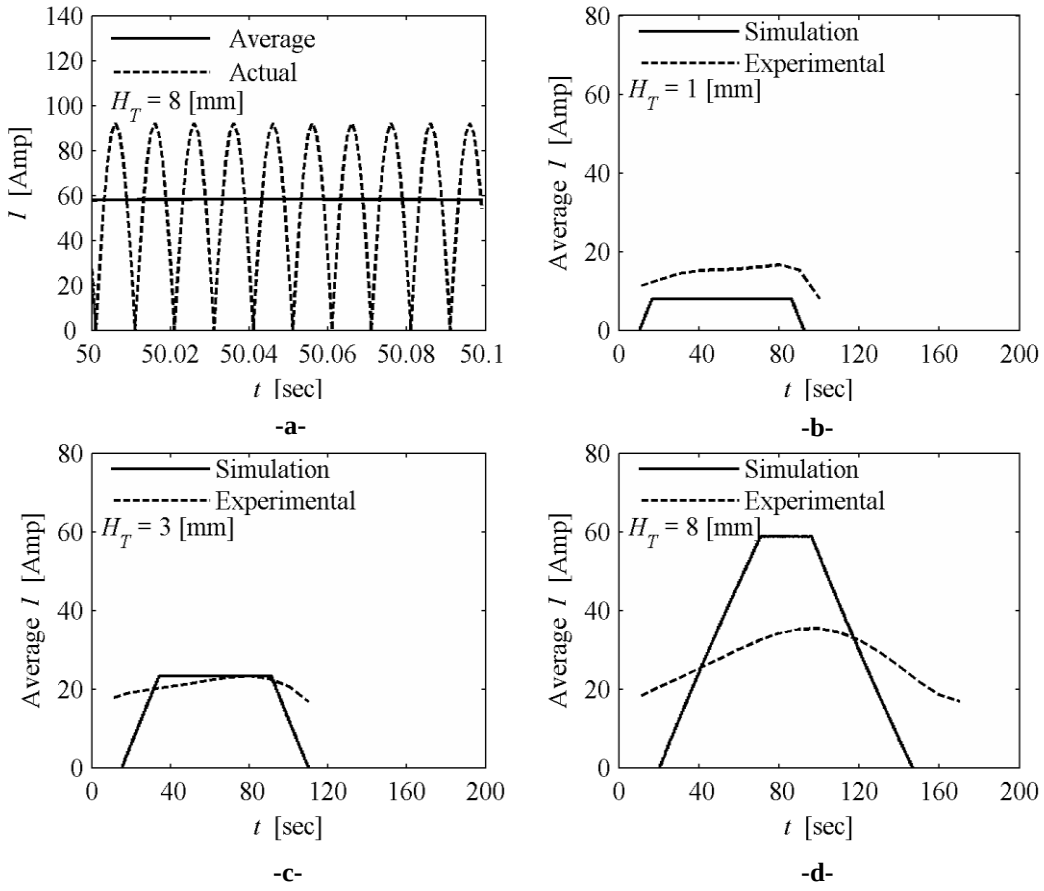

Fig. 5. Experimental and simulated machining current.

Fig. 6 shows the simulated effect of work part orbiting speed, *N*, on volumetric and linear removal rates, *VRR* and *LRR*, respectively, and hole inaccuracy as represented by straightness and roundness errors. From fig. 6-a, it is clear that the effect of *N* on *VRR* and *LRR* is marginal. However, the effect of N on straightness and roundness errors is significant, especially at small *N*. Increasing *N* results in a decrease in roundness and straightness errors. This is due to the averaging action of the orbital motion of the tool on the machining rate at the surface of the hole and consequently on R_W. Also, figs 6-a and 6-b show that the effect of feedrate on straightness and roundness errors is negligible. In the same figure, the feedrates are expressed as mm/min rather than mm/rev as there are variations in *N*.

Fig. 7-a shows the simulated effect of tool radius, R_T, on volumetric and linear removal rates, *VRR* and *LRR*, respectively. From the figure, it can be seen that increasing R_T results in decreasing *VRR* and *LRR* up to R_T= 3 mm. Increasing R_T, beyond 4 mm, results in an increase of *VRR* and *LRR*. An explanation of this result can be given in terms current density distribution which is shown in fig.7-b. The current density distribution for R_T=4 mm is determined at an arbitrary cross section of the work part at an arbitrary time during machining. It is represented by the dashed line in the figure. Obviously it is much lower compared with the current density distributions of for R_T=0.5 and for R_T=7 mm.

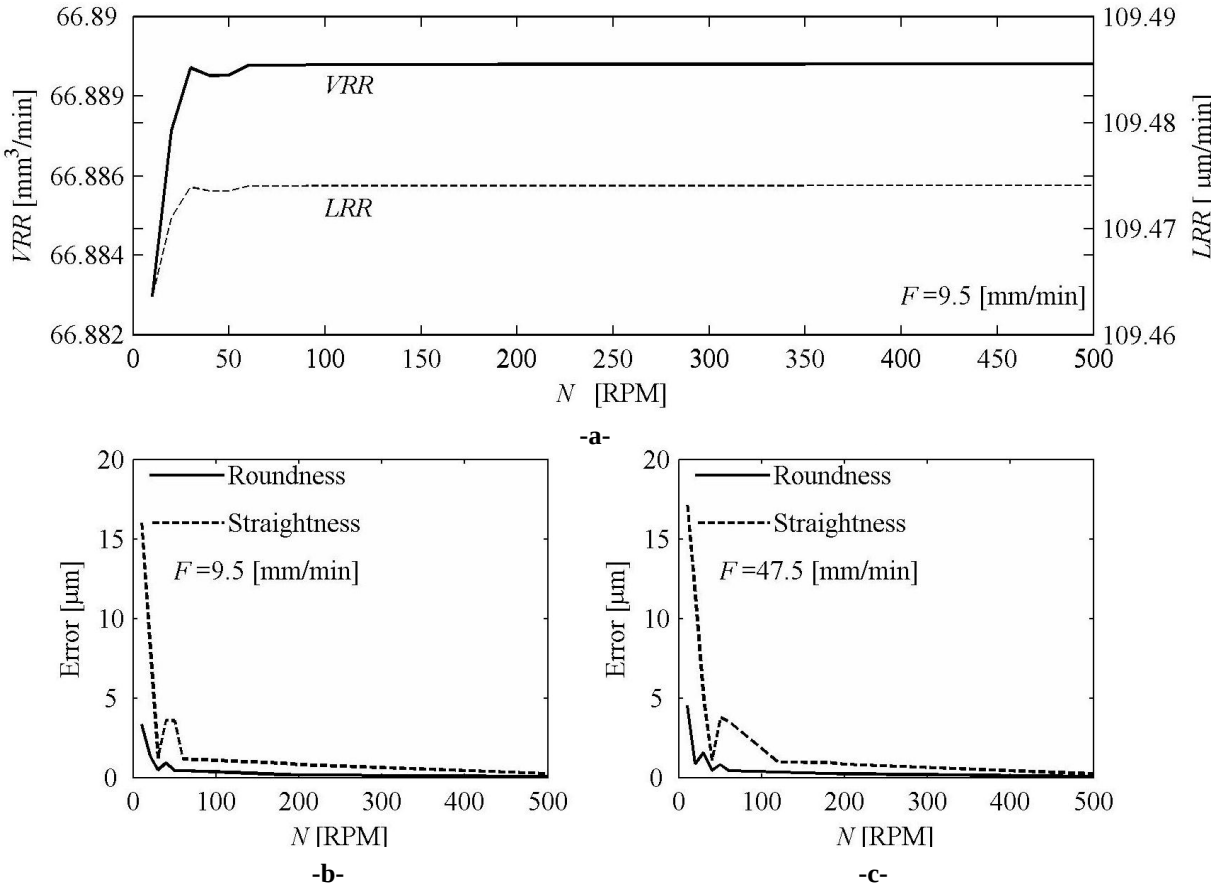

Fig. 6. Simulated effect of work part orbiting speed, *N*, on volumetric and linear removal rates, *VRR* and *LRR*, respectively, and hole inaccuracy.

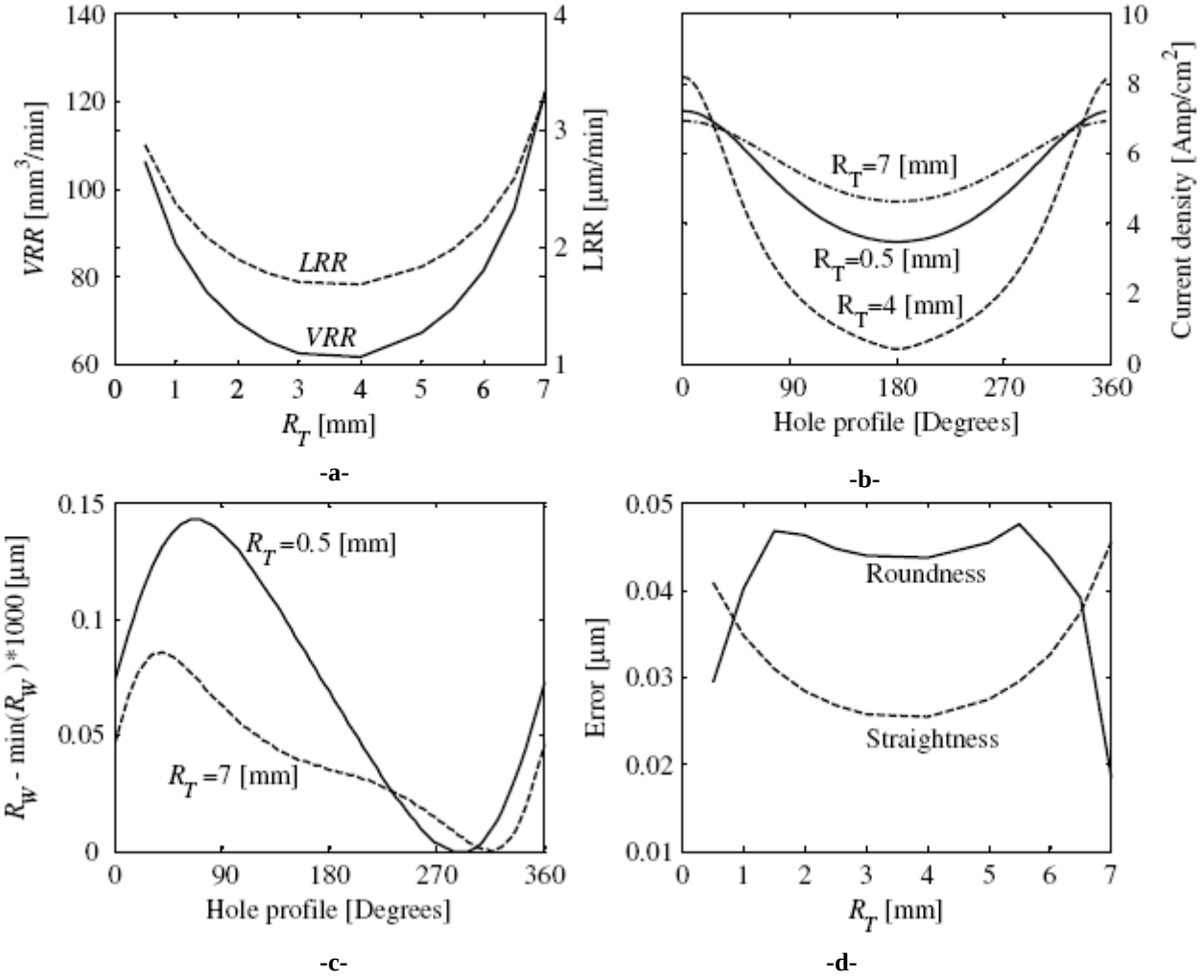

Fig. 7. Effect of tool radius, R_T, on volumetric and linear removal rates, *VRR* and *LRR* and hole inaccuracy.

Fig. 7-c shows the variations in R_W for R_T equal to 0.5 and 7 mm. The data is obtained from a cross section at the bottom of the work part, fig.1 or at the far left side of the work part, fig. 2-a. The variation in R_W using the tool with R_T = 4 mm is smaller compared with that using the tool having R_T = 4 mm. Also, straightness is minimum when using the tool with R_T = 4 mm. However, the roundness error, when using the tool with R_T = 4, is larger.

The simulated effect of tool eccentricity, *E*, on volumetric and linear removal rates, *VRR* and *LRR*, respectively, is shown in fig. 8-a. From the figure, it can be seen generally that increasing *E* increases *VRR* and *LRR*. However, for smaller *E*, the increase is minor, while, for larger *E*, the increase in larger. This is because increasing *E* results in a corresponding decrease in the machining gap and consequently more machining. The effect of *E* on straightness and roundness errors are shown in fig. 8-b, which indicates that roundness error is more susceptible to *E* compared with straightness error. This can be reduced to fact that *E* varies in radial direction and consequently it has more effect on roundness error.

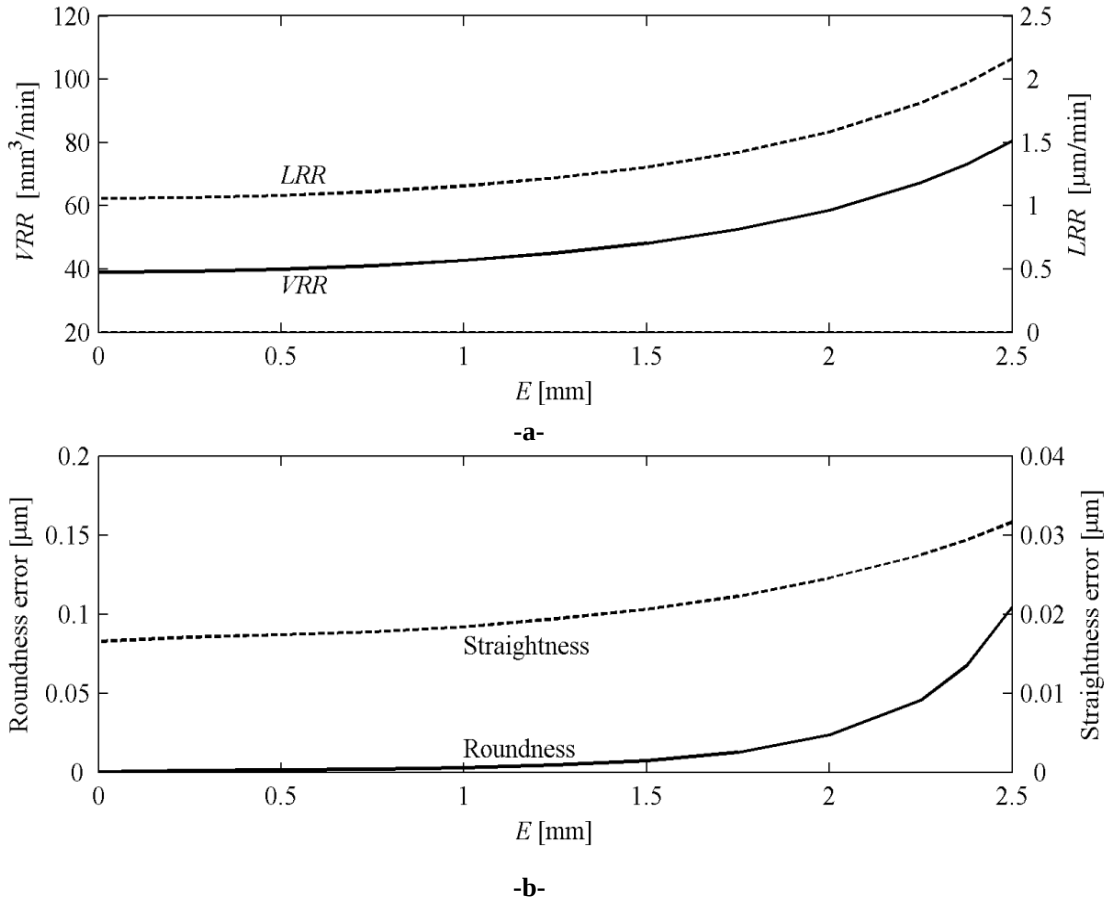

Fig. 8. Effect of tool eccentricity, *E*, on volumetric and linear removal rates, *VRR* and *LRR*, respectively, and hole inaccuracy.

5. Conclusions

This work presents a model for the orbital electrochemical hole sizing process; using feeding tools. The model was used to investigate the correlation between different process parameters and process performance measures. The effect of feedrate on volumetric metal removal rate and linear removal rate was found to be marginal; a conclusion that was verified experimentally. Also, it was found that the effect of orbiting speed on volumetric removal rate and linear removal rate is negligible compared with its effect on hole inaccuracy as represented by roundness and straightness errors. Increasing orbiting speed resulted in reduced hole roundness and straightness errors. Moreover, it was found that small or large tool radius should be used to ensure large volumetric removal rate and low hole inaccuracy. A certain range of tool radius should actually be avoided as it results in small volumetric removal rate and large hole inaccuracy. Finally, increasing tool eccentricity resulted in increasing volumetric removal rate and linear removal rate. However, it led to an increase in hole inaccuracy.

References

[1] H. El-Hofy, Advanced Machining Processes, Non-traditional and Hybrid Processes, McGraw Hill. Corporation, New York, USA, ISBN 0-07-145334-2 (2005).

[2] K.P. Rajurkar and D. Zhu, "Improvement of Electrochemical Machining Accuracy by Using Orbital Electrode Movement", Annals of the CIRP, Vol. 48 (1), pp. 139-142 (1999).

[3] J. Kozak, K.P. Rajurkar and R. Balkrishna, "Study of Electrochemical Jet Machining Process", Transactions of the ASME, Vol. 118, pp. 490-498 (1996).
[4] Mohen Sen and H.S. Shan, "A review of Electrochemical Macro- to Micro-Hole Drilling Processes. International Journal of Machine Tools and Manufacture, Vol. 45, pp.137-152 (2005).
[5] S. Sharma, V.K. Jain and R. Shekhar, "Electrochemical Drilling of Inconel Superalloy with Acidified Sodium Chloride Electrolyte", International Journal of Machine Tools and Manufacture, Vol. 19, pp. 492-500 (2002).
[6] H. Hocheng and P.S. Pa, "Electropolishing and Electrobrightening of Holes Using Different Feeding Electrodes", Journal of Materials Processing Technology, pp. 89-90: 440-446 (1999).
[7] T. Masuzawa and S. Sakai, "Quick Finishing of WEDM Products by ECM Using Mate Electrodes", Annals of the CIRP, Vol. 36 (1), pp. 123-126 (1999).
[8] J. Kozak, L. Dabrowiski and H. Osman, "Computer Modelling with Rotating Electrode", Journal of Materials Processing Technology, Vol. 28, pp. 157-167 (1991).
[9] M.S. Hewidy, S.J. Ebied, K.P. Rajurkar and M.F. El-Safti, "Electrochemical Machining Under Orbital Motion Conditions", Journal of Materials Processing Technology, Vol. 109, pp. 339-346 (2001).
[10] Z. Sadollah Bamerni and H. El-Hofy, "Orbital Electrochemical Machining of Electrodischarge Machined Surfaces. Advanced Manufacturing Systems and Technology", CIST Courses Lectures No. 437, pp. 464-487 (2002).
[11] H. El-Hofy, N. Al-Salem and M. Abd-ElWahed, "Orbital Electrochemical Finishing of Holes Using Stationary Tool", CAPE-10, 18-19 March, Edinburgh, Scotland, pp. 169-177 (2003).
[12] N. Al-Salem, H. El-Hofy and M. AbdElWahed, "Orbital Electrochemical Hole Finishing Using Feeding Tools", AlAzhar Engineering 7th International Conference, pp. 7-10 April (2003).
[13] H. El-Hofy, "Computer Aided Design of Tool Shape for EC-Sizing of EC-Drilled Holes", Alexandria Engineering Journal, Vol. 28 (3), pp. 383-402 (1989).
[14] J.FW. Galyer and C.R ShotBolt, "Metrology for Engineers", Cassell Publishers Ltd, ISBN 0 304 317 34 9 (1990).

Received May 29, 2007
Accepted October 16, 2007